

THERMAL PROPERTIES OF SOME COMPOSITIONS IN THE CHALCOGENIDE SYSTEM $Sb_{40}Te_{60-x}Se_x$

M. M. Ibrahim, M. M. Wakkad, E. Kh. Shokr and H. A. Abd-El-Ghani

PHYSICS DEPARTMENT, FACULTY OF SCIENCE (SOHAG), ASSIUT UNIVERSITY,
SOHAG, EGYPT

(Received November 20, 1990)

The thermal diffusivities, specific heats and thermal conductivities of the binary compositions $Sb_{40}Te_{60}$ and $Sb_{40}Se_{60}$ and the ternary composition $Sb_{40}Te_{30}Se_{30}$ were measured in the range ~ 320 to 500 K. It was found that the environmental temperature, the content of Se in the composition and the conditions of measurements are decisive factors greatly influencing both the values and the behaviour of the thermal parameters, and the mechanisms of thermal transport. Although the tested compositions exhibit semiconducting behaviour, the free charge carrier component of the thermal conductivity was so small as to be negligible. Thus, it could be concluded that the observed thermal conductivity is attributable to both photon and phonon mechanisms.

Measurements of thermal properties, and especially the thermal conductivity, of chalcogenide materials containing one or more of the chalcogen elements Se, Te and/or S, have proved of interest [1-5]. Yokota and Katayama [1] have measured the thermal conductivities of the semiconducting alloy systems $((Bi_{1-x}Sb_x)_2Te_3$ and $Bi_2(Te_{1-y}Se_y)_3$ with $0 \leq x, y \leq 1$ in the cleavage planes, in the temperature range from 90 to 300 K. They proved that the heat conduction by charge carriers is smaller than that by phonons, and the heat conduction due to the simultaneous thermal diffusion of electrons and holes is as important as the lattice thermal conduction at temperatures near 300 K. They also obtained both the harmonicity and the disorder parameter from the lattice thermal conductivity, by using the Klemens-Callaway theory. Consideration of the relations between the anharmonicity and the disorder parameter leads to the conclusion that the three-phonon processes are modified by point defects, and the phonon-phonon

interaction of the type $a + a \rightleftharpoons o$ participates in the lattice thermal conduction, where a and o refer to the acoustic and optical phonons, respectively.

The composition dependence of the lattice thermal conductivity of $\text{Bi}_{2-z}\text{Sb}_z\text{Te}_{3-x-y}\text{Se}_x\text{S}_y$ solid solutions in the range $0 \leq x + y \leq 0.9$ (with $x/y = 1$) and $0 \leq z \leq 0.6$ was studied by Bekurdyev *et al.* [2]. They proved that the introduction of Sb, Se and S atoms results in an additional fall in the lattice thermal conductivity, which is attributable to the different masses of the atoms participating to the substitution and to different changes in the elastic forces.

The effect of structure on the thermal conductivity was tested by Boikov *et al.* [3] on films prepared by discrete evaporation in vacuum of the chalcogenides Bi_2Te_3 , $\text{Bi}_{0.5}\text{Sb}_{1.5}\text{Te}_3$ and $\text{Bi}_2(\text{Te},\text{Se})_3$. The use of different substrates allowed films with different internal structures to be prepared and studied. However, it was found that the phonon scattering at the grain boundaries has a substantial effect on the thermal conductivity. The lattice thermal conductivity of the films was considerably lower than that of bulk crystals with similar compositions. The rapid increase in the lattice thermal conductivity with crystal grain size showed that the phonon scattering at the grain boundaries is responsible for the lower thermal conductivity of the films. Further, the effect of the boundary scattering of phonons on the thermal conductivity of Bi_2Te_3 films is much less than that for $\text{Bi}_{0.5}\text{Sb}_{1.5}\text{Te}_3$ films, which demonstrates the different roles of long-wavelength phonons in the thermal conductivities of the two materials. In addition, the results of the investigation of the thermal conductivity of fine-grained $\text{Bi}_{0.5}\text{Sb}_{1.5}\text{Te}_3$ films obtained by Abduraimov *et al.* [4] allowed the same conclusion that long-wave-length phonons make a considerable contribution in materials based on bismuth and antimony chalcogenides.

The aim of the present work was to investigate the effects of the environmental temperature, T (in the range ~ 320 -500 K), and heat treatment on the thermal diffusivity, a , specific heat, C_p , and thermal conductivity, k , of some compositions in the alloy system Sb-Te-Se.

Experimental technique

The working compositions were prepared from elemental Sb, Te and Se of 99.999% purity. The appropriate amounts of the elements were mixed together in a silica tube which was sealed after evacuation to 10^{-4} Torr. The mixture was melted at 800° for about 12 h. The charged ampoule was oc-

asionally agitated by rocking the furnace to ensure the homogeneity of the melt. The melt was then quenched at 0° in ice-water. The X-ray diffraction analysis (XRD) proved that this method results in the preparation of polycrystalline compositions.

Cutting, polishing and washing techniques were used for the preparation of samples in disc form with highly polished and flat surfaces.

The non-steady state or plane thermal wave method was used for simultaneous measurements of thermal diffusivity, specific heat and thermal conductivity. The experimental set-up and methods of analysis and calculations were basically as described in detail elsewhere [6-9]. Measurements of thermal properties were performed under a pressure less than 10^{-5} Torr. A perturbation heater was sandwiched in between the test specimen and a pure copper standard one. Measurable oscillating temperature amplitudes of the outer surface of the test specimen could be obtained with a chromel-alumel thermocouple by adjusting the sandwiched perturbation heater power. The time-dependent component and the on-off signals of the perturbation heater power were displayed on a sensitive recorder.

The time-dependent component of temperature, $T(x,t)$ K, set up in the specimen satisfies the following one-dimensional heat equation [8]:

$$\frac{\partial^2 T}{x^2} = a^{-1} \frac{\partial T}{\partial t} \quad (1)$$

Via some mathematical manipulations [6, 9], the thermal diffusivity can be calculated, since

$$a = \frac{\omega l^2}{\chi(B, \Phi)} \quad (2)$$

where ω is the angular frequency of the perturbed heater power, l is the thickness of a test sample and $\chi(B, \Phi)$ is a function of both the phase shift angle, Φ , between the input heating power and the oscillating temperature of the outer surface of the test sample and the heat loss parameter, B , which is called the Biot number. The parameter B represents the ratio between the internal thermal resistance to conduction and the external resistance to heat transfer.

The technique adopted for the determination of B is that of running two tests for two frequencies on the same sample (one frequency is double the

other). The two phase shift angles $\Phi(\omega)$ and $\Phi(2\omega)$ will meet on one of the theoretical curves of different Biot numbers.

The expression for specific heat can be written as

$$C_p = \frac{2IV}{\pi m w T_{\max}} \eta(\chi, B) \quad (3)$$

where V is the voltage applied to the perturbation heater, I is the current flowing in the half period of the first harmonic, m is the mass of the test sample, T_{\max} is the amplitude of the oscillating temperature of the outer surface of the sample, and $\eta(\chi, B)$ is a correction function for T_{\max} and is equal to the ratio between the amplitudes of the oscillating temperatures of the outer and inner surfaces of the test sample. The mathematical analysis proves that $\eta(\chi, B)$ is a function of the Biot number B . Hence, η can be drawn [6] vs. the function η determined for the thermal diffusivity evaluation, for different values of B .

Via the density of the sample, d , the thermal conductivity can be calculated, since

$$k = a C_p d \quad (4)$$

The experimental errors in the thermal properties measured with this method did not exceed 4.5% for a , and 4% for C_p .

Results and discussion

Effect of composition

Figure 1 shows the variations in a , C_p and k (measured at ~ 348 K) with selenium content in the system $\text{Sb}_{40}\text{Te}_{60-x}\text{Se}_x$ for virgin specimens and for specimens annealed at 340° for 32 h. The data in Fig. 1. indicate that each of the three thermal parameters possesses a maximum value at the composition $\text{Sb}_{40}\text{Te}_{45}\text{Se}_{15}$. All exhibited a continuous decrease with further enrichment with Se up to 60 at.%. The observed increases in a , C_p and k with increase of the content of Se from 0 to 15 at.% can be attributed to the relatively high values of the thermal parameters characterizing selenium with respect to those for tellurium [10]. On the other hand, the decreases in these thermal parameters with further increase of the Se content in the compositions was due to the decrease in the tellurium content, which has the highest atomic

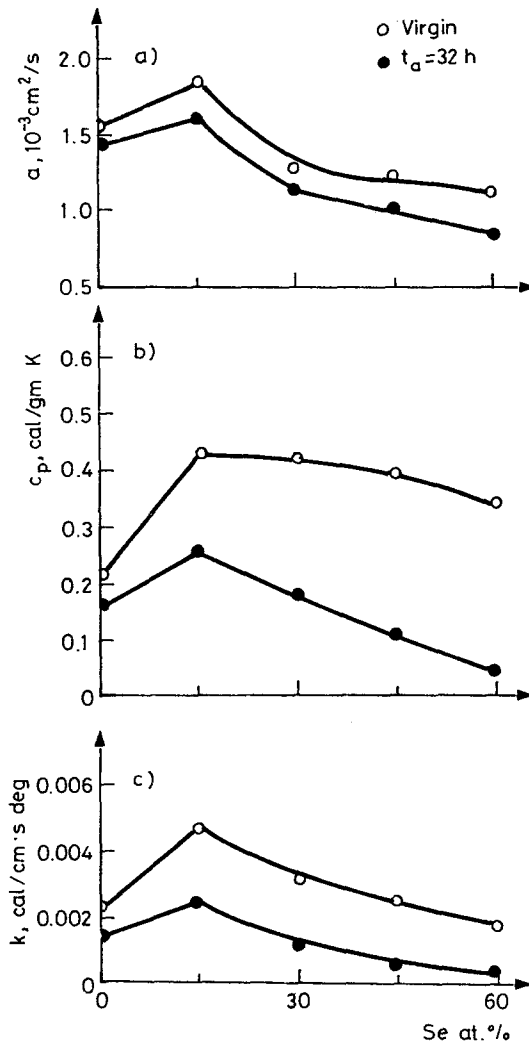


Fig. 1 Variation of (a) thermal diffusivity, (b) specific heat and (c) thermal conductivity with Se content in the compositions

weight (127.61) [10] from among the three elements forming the system $\text{Sb}_{40}\text{Te}_{60-x}\text{Se}_x$; this results in turn in a decrease in the density of the compositions. The observed decreases in the thermal parameters with annealing could be attributed to the greater harmonicity of the lattice vibrations associated with crystallization and recrystallization of the test sample, as proved previously [7].

Effect of ambient temperature

The temperature dependences of a , C_p and k for virgin specimens of the compositions $Sb_{40}Te_{60}$, $Sb_{40}Te_{30}Se_{30}$ and $Sb_{40}Se_{60}$, and for specimens annealed at 340° for 16 and 32 h, were studied in the range ~ 320 – 500 K. It may be

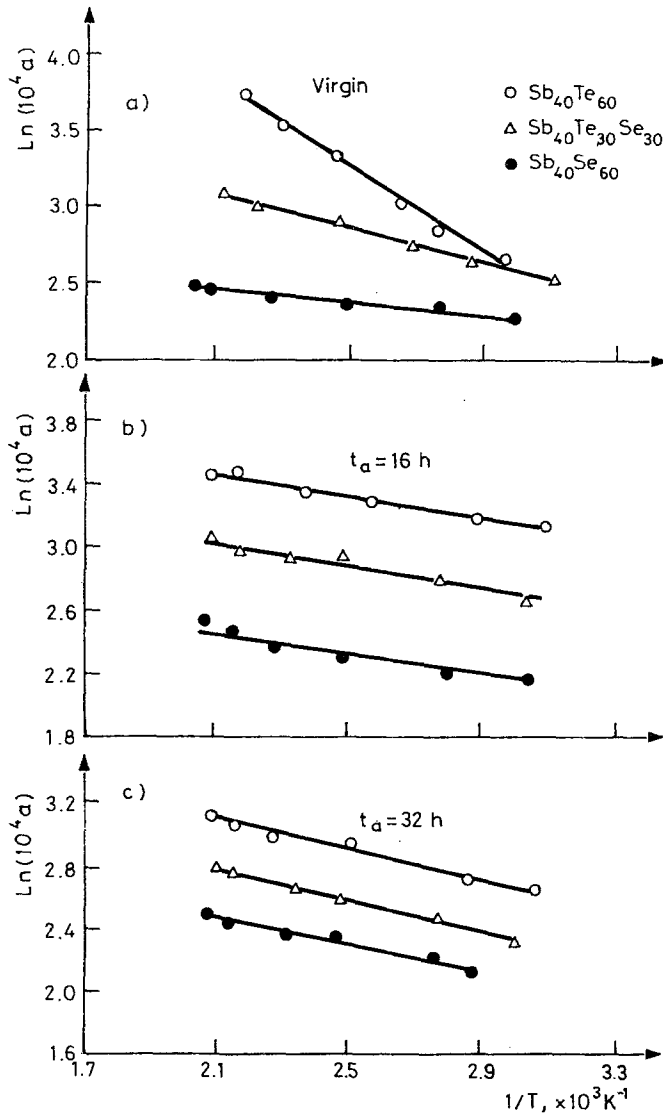


Fig. 2 The $\ln a - 1/T$ relations for (a) as-prepared, (b) annealed for 16 h and (c) annealed for 32 h compositions. $T_a = 340^\circ\text{C}$

seen in Figs 2–4 that the three parameters a , C_p and k increased with increasing T , decreased with Se enrichment and also decreased with annealing and with prolongation of the annealing time. In addition, the $\ln L$ vs. $1/T$ plots (L can refer to any of the three thermal parameters) were linear, suggesting the following Arrhenius-like equation:

$$L = L_0 e^{-E_1/k_B T} \quad (5)$$

where L_0 represents the pre-factor or temperature-independent value of L , while K_B is the Boltzmann constant, and E_1 is the activation energy for a particular mechanism which contributes to a certain thermal parameter.

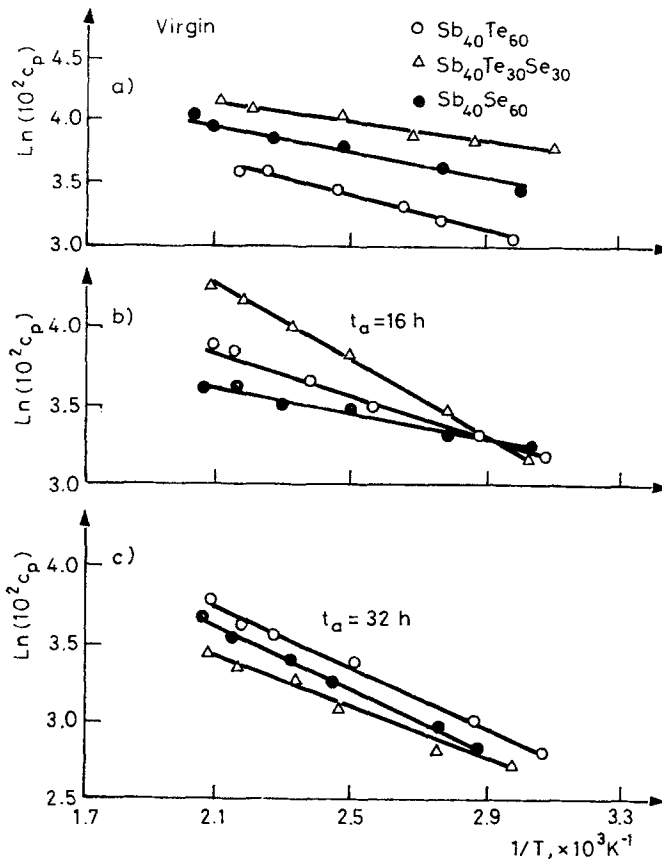


Fig. 3 The $\ln C_p - 1/T$ relations. a, b and c as in Fig. 2 $T_a = 340^\circ\text{C}$

The plots in Figs 2-4 gave the values listed in Table 1 for the activation energies and pre-factors.

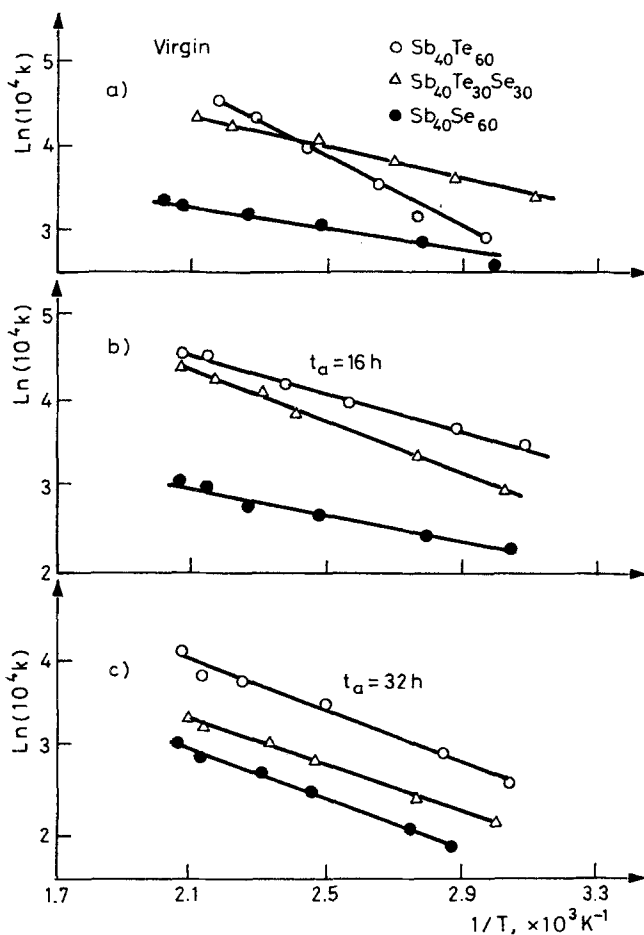


Fig. 4 The $\ln k - 1/T$ relations. a, b and c as in Fig. 3 $T_a = 340^\circ\text{C}$

The most characteristic feature of the results in Table 1 is that the changes in both E_1 and L_0 with change of the conditions of heat treatment are not sequential. This can be related to unsystematic changes in microstructure, which result in turn in unsystematic variations in the modes of mechanisms of phonons scattering on annealing. However, the changes in the microstructure of the samples with these compositions on annealing were studied earlier [7, 11].

Table 1 Values of the corresponding activation energies (E_a , E_{cp} and E_k) and pre-factors (a_o , C_{po} and k_o)

Composition t_a (h)	Sb ₄₀ Te ₆₀			Sb ₄₀ Te ₃₀ Se ₃₀			Sb ₄₀ Se ₆₀		
	E_a , eV	a_o , cm ² /s	E_a , eV	a_o , cm ² /s	E_a , eV	a_o , cm ² /s	E_a , eV	a_o , cm ² /s	
Virgin	0.116	0.0750	0.047	0.0071	0.016	0.0018			
16	0.028	0.0063	0.028	0.0041	0.029	0.0024			
32	0.038	0.0057	0.041	0.0045	0.034	0.0028			
Virgin	E_{cp} , eV	C_{po} , cal/gmdeg	E_{cp} , eV	C_{po} , cal/gmdeg	E_{cp} , eV	C_{po} , cal/gmdeg			
16	0.062	1.8200	0.030	1.3000	0.046	1.640			
32	0.061	2.1100	0.100	7.8500	0.033	0.830			
Virgin	E_k , eV	k_o , cal/cmSdeg	E_k , eV	k_o , cal/cmSdeg	E_k , eV	k_o , cal/cmSdeg			
16	0.082	3.0300	0.072	1.7500	0.083	2.750			
32	0.178	0.8139	0.078	0.0529	0.032	0.0058			
Virgin	0.088	0.0793	0.127	0.1816	0.062	0.0091			
16	0.120	0.1024	0.113	0.0451	0.117	0.0346			
32									

Table 2 Values of activation energy of electrical conduction, E_{σ} , and thermoelectric power, E_s , for virgin specimens in the system $Sb_{40}Te_{60-x}Se_x$ and for specimens annealed at 340°

Composition t_a (h)	E	$Sb_{40}Te_{60}$	$Sb_{40}Te_{45}Se_{15}$	$Sb_{40}Te_{30}Se_{30}$	$Sb_{40}Te_{15}Se_{45}$	$Sb_{40}Se_{60}$
Virgin	E_{σ} , eV	-	-	0.008	0.069	0.127
16	E_{σ} , eV	-	-	0.016	0.073	0.047
Virgin	E_s , eV	0.111	0.071	0.250	0.030	0.598
16	E_s , eV	0.160	0.160	0.100	0.020	0.104
32	E_s , eV	0.020	0.192	0.270	0.010	-

In comprehensive work, the temperature dependence of both the electrical conductivity and the thermoelectric power of the present compositions have been studied [7, 11]. The values obtained for the activation energies of electrical conduction, E_{σ} , and thermoelectric power, E_s , were as recorded in Table 2.

From a comparison of the results in Tables 1 and 2, it could be concluded that the activation energy values deduced from the temperature dependence of any of the three considered thermal parameters are approximately one order of magnitude higher than those deduced from the temperature dependence of either the electrical conductivity or the Seebeck coefficient. This might reveal firstly that the mechanisms contributing to the thermal properties are quite different from those contributing to the electrical transport properties, and secondly that the role of the contribution of charge carriers to the thermal transport behaviour of these compositions is either very weak or entirely absent. At first sight, this might prove that the thermal transport processes mainly involve the participation of phonons; this will be returned to later.

With the corresponding values for the d.c. electrical conductivity [7, 11], the electronic component of the thermal conductivity, k_e , is calculated by using the following equation:

$$k_e = L'T\sigma \quad (6)$$

where L' is the Lorentz number, considered to be equal to $0.3563 \cdot 10^{-8}$ cal Ω deg $^{-2}$ s $^{-1}$ for semiconductors [12] and σ is the electrical conductivity. Table 3 gives the values calculated for k_e .

Table 3 The electronic component of thermal conductivity, k_e , for some compositions in the system $\text{Sb}_{40}\text{Te}_{60-x}\text{Se}_x$

Composition	$\text{Sb}_{40}\text{Te}_{60}$	$\text{Sb}_{40}\text{Te}_{45}\text{Se}_{15}$	$\text{Sb}_{40}\text{Te}_{30}\text{Se}_{30}$	$\text{Sb}_{40}\text{Te}_{15}\text{Se}_{45}$	$\text{Sb}_{40}\text{Se}_{60}$
$k_e 10^{-8}$ cal/cmS deg					
as-prepared	593	349	186	202	3.55
$T_a = 340^\circ\text{C}$					
$t_a = 16$ h	0.335	0.283	0.163	0.190	0.248

The data in Table 3, together with those in Fig. 4, prove that the values for k_e are about three orders of magnitude (in the case of as-prepared specimens) or about six orders of magnitude (in the case of heat-treated

specimens) smaller than those of the measured or total thermal conductivities of the considered compositions. This conclusion proves beyond doubt that the component of thermal conductivity due to charge carriers is so small as to be negligible.

Mode of thermal transport

The power of the absolute measuring temperature is a decisive means of identifying the main mechanism contributing to scattering. Therefore, the data in Fig. 4 were reconfigured in the form of $\ln k$ vs. $\ln T$ plots, as shown in Fig. 5. The plots are linear, verifying that the measured thermal conductivity is directly proportional to T^n . Values of n were calculated and are listed in Table 4.

Table 4 Variation in the power n with time of annealing and selenium content in the compositions

Composition t_a (h)	Sb ₄₀ Te ₆₀	Sb ₄₀ Te ₃₀ Se ₃₀	Sb ₄₀ Se ₆₀
Virgin	5.23	2.31	1.78
16	2.61	3.73	1.83
32	3.51	3.29	3.32

All values in Table 4 for the power n exceed unity. However, for the Te free composition, the values of n increased continuously on annealing and prolongation of the annealing time. For the Se free composition, while the value of n was decreased by annealing, it was increased by prolongation of the annealing time. For the composition containing both Te and Se, the value of n was increased by annealing for 16 h, and then slightly decreased on prolongation of the annealing time to 32 h. The variation in n with variation of the conditions of sample preparation can be interpreted in terms of the changes in the modes of phonon scattering resulting from the corresponding changes in the internal microstructure of a sample with a particular composition. Further, the observed increase in n might be regarded as due to a decrease in the point defect concentration. This could be justified from microstructural examinations [7, 11].

For these compositions, the component of thermal conductivity due to charge carriers is presumed to be so small as to be negligible. Accordingly [13], the lattice conduction is characterized by a lattice thermal conductivity, k_1 . Radiative thermal transport in samples of material which are optically

thick is governed, for small temperature gradients, by a radiative conductivity, k_r , which is given by

$$k_r = 16 \frac{\delta n^2 T^3}{3 \bar{\epsilon}} \quad (7)$$

where δ is the Stefan-Boltzmann constant, n is the refractive index (assumed to be wavelength-independent), and $\bar{\epsilon}$ is the mean black body extinction

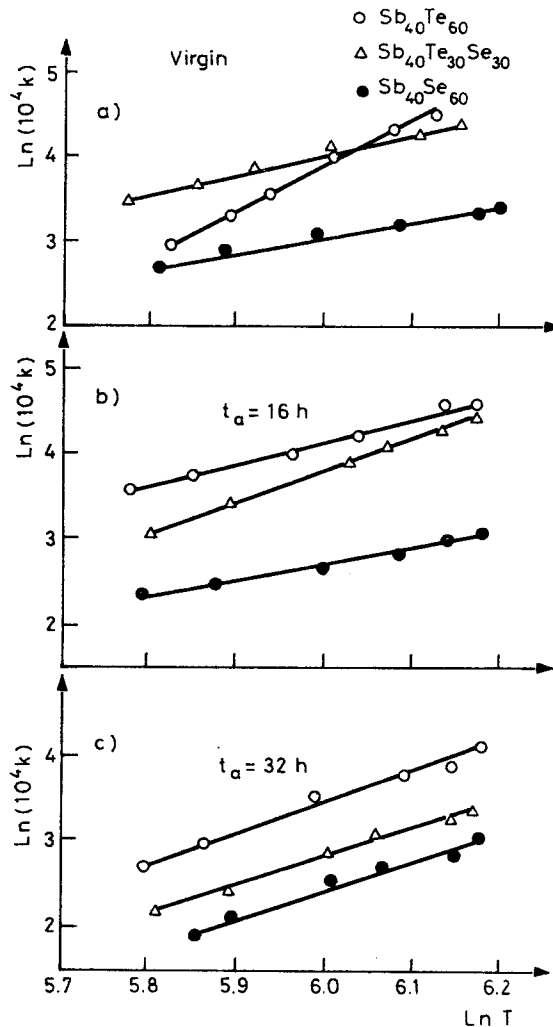


Fig. 5 The $\ln k$ - $\ln T$ relations. a, b and c as in Fig. 4 $T_a = 340^\circ\text{C}$

coefficient. A sample is optically thick if $\bar{\epsilon}l > 1$, where l is the sample thickness. Both lattice and radiative thermal conductivities are additive, and therefore

$$k = k_1 + k_r \quad (8)$$

Equation (7) indicates that the radiative component of thermal conductivity increases according to a T^3 law. On the other hand, it has to be remembered that, for lattice thermal conductivity, in the range $T < \Theta$, where Θ is the Debye temperature, $k_1 \sim T^3$, while in the high-temperature range $T > \Theta$, the lattice thermal conductivity is inversely proportional to the temperature, i.e. $k_1 \sim T^{-1}$. Therefore, it can be concluded that the increment in thermal conductivity of the present compositions with temperature proves that the Debye temperatures of these compositions have not been reached. On the other hand, exceeding the value 3 for the power n of the absolute temperature might prove that both lattice and radiative or photon components of thermal conductivity contribute additively. The highest contribution of the radiative component of thermal conductivity is expected for thermally untreated samples of the composition $\text{Sb}_{40}\text{Te}_{60}$. The discrepancy in the values of n from the value 3 while k still increases with increasing T might indicate that the Debye temperature is not extremely exceeded in a way that normal three-phonon and Umklapp processes and phonon scattering processes by point defects are all probably involved.

Conclusions

The thermal parameters of the considered compositions in the system $\text{Sb}_{40}\text{Te}_{60-x}\text{Se}_x$ are greatly dependent on both the selenium content and the conditions of heat treatment. The temperature dependence of each of the three considered thermal parameters can be fully described by an Arrhenius-like equation. Both phonons and photons contribute to the observed total thermal conductivity. In addition, the role of microstructural changes is significant.

References

- 1 K. Yokota and S. Katayama, *Jap. J. Appl. Phys.*, 12 (1973) 1205.
- 2 Ch. D. Bekdurdyev, B. M. Gol'tsman and V. A. Kutasov, *Sov. Phys. Solid State*, 16 (1975) 1790.

- 3 Yu. A. Boikov, B. M. Gol'tsman and V. A. Kutasov, *Sov. Phys. Solid State*, 20 (1978) 757, *ibid* 20 (1978) 1733.
- 4 V. E. Abduraimov, Yu. A. Boikov and V. A. Kutasov, *Sov. Phys. Solid State*, 26 (1984) 1636.
- 5 N. A. Red'Ko, M. P. Boiko, N. A. Rodionova and V. I. Pol'Shin, *Sov. Phys. Solid State*, 29 (1987) 1627.
- 6 M. M. Wakkad, M. Sc. Thesis, Faculty of Science, Assiut University, Assiut, Egypt 1979.
- 7 H. A. Abd-El-Ghani, M. Sc. Thesis, Faculty of Science (Sohag), Assiut University, Sohag, Egypt 1989.
- 8 H. S. Carslaw and J. C. Jaeger, *Conduction of Heat in Solids*, (2nd Ed.) Oxford University, New York, 1959.
- 9 R. D. Cowan, *J. Appl. Phys.*, 32 (1961) 1363, *ibid* 34 (1963) 926.
- 10 R. B. Ross, *Metallic Materials Specification Handbook E* and F. N. Spon Ltd, London 1972 pp. 349, 661.
- 11 M. M. Ibrahim, M. M. Wakkad, E. Kh. Shokr and H. A. Abd-El-Ghani, *Bull. Fac. Sci. (Sohag) Assiut University*, 5 (1989) 385, *ibid* 5 (1989) 279.
- 12 G. I. Epifanov, *Solid State Phys.*, Mir, USSR 1979, p. 176.
- 13 J. Schatz and G. Simmons, *J. Appl. Phys.*, 43 (1972) 2586.

Zusammenfassung — Im Temperaturbereich 320-500 K wurde das Temperaturleitvermögen, die spezifische Wärme und die Wärmeleitfähigkeit der binären Kompositionen $Sb_{40}Te_{60}$ bzw. $Sb_{40}Se_{60}$ und der ternären Komposition $Sb_{40}Te_{30}Se_{30}$ untersucht. Man fand, daß die Umgebungstemperatur, der Se-Gehalt der Kompositionen und die Meßbedingungen entscheidende Faktoren sind, welche sowohl Wert als auch Verhalten der thermischen Parameter, weiterhin den Mechanismus des Wärmetransportes beeinflussen. Obwohl die untersuchten Kompositionen Halbleiterverhalten zeigten, war die freie Ladungsträgerkomponente der Wärmeleitfähigkeit so gering, daß sie vernachlässigt werden konnte. Somit konnte darauf geschlossen werden, daß die beobachtete Wärmeleitfähigkeit sowohl Photonen- als auch Phononenmechanismen zugeschrieben werden kann.